Experimental and Theoretical Investigation of Simple Terminal Group 6 Arsenide As≡MF_3 Molecules

Xuefeng Wang,[†] Lester Andrews,*[,†] Marta Knitter,[‡] Per-Åke Malmqvist,[‡] and Björn O. Roos[‡]

Department of Chemistry, University of Virginia, Charlottesville, Virginia 22904-4319, and Department of Theoretical Chemistry, Chemical Center, University of Lund, P.O. Box 124, 2-221 00 Lund, Sweden

Received: February 12, 2009; Revised Manuscript Received: March 31, 2009

Laser-ablated group 6 metal atoms react with NF_3 and PF_3 to form the simple lowest energy N≡MF_3 and P≡MX_3 products, and this investigation has been extended to AsF_3. Mo and W atoms react with AsF_3 upon excitation by laser ablation or UV irradiation to form stable trigonal As≡MF_3 terminal arsenides. These molecules are identified by comparison of the closely related infrared spectra of the analogous phosphide species and with frequencies calculated by density functional theory and multiconfigurational second order perturbation theory (CASSCF/CASPT2). Computed CASSCF/CASPT2 triple bond lengths for the As≡MoF_3 and As≡WF_3 molecules are 2.240 Å and 2.250 Å, respectively. The natural bond orders calculated by CASSCF/CASPT2 decrease from 2.67 to 2.60 for P≡MoF_3 to As≡MoF_3 and from 2.74 to 2.70 for P≡WF_3 to As≡WF_3 as the arsenic valence orbitals are less effective than those of phosphorus in bonding to each metal atom and the larger metal orbital size becomes more compatible with the arsenic valence orbitals. The Cr atom reaction gives the arsinidene AsF=CrF_2 product instead of the higher energy As≡CrF_3 molecule as the Cr (VI) state is not supported by the softer pnictides.

Introduction

Transition metal complexes containing metal nitride and phosphide terminal groups have been investigated extensively. The heavier transition metal nitrides were synthesized first, and analogous phosphide complexes have followed.[1] However, there are very few examples of terminal arsenide complexes.[2−4] The first arsenide complex to be prepared, [(N_3N)W≡As], revealed a W≡As bond length of 2.29 Å.[2]

The organometallic chemistry of terminal triple bonds has many applications. Catalytic nitrile metathesis for L_3MoN and L_xWN systems has been investigated by the Johnson group.[4−6] This chemistry has been extended to terminal phosphide functional groups by Cummins and co-workers to investigate and employ alkoxide stabilized Mo≡P triple bonds and terminal nitride-to-phosphide conversions.[8−12] Most of the above chemistry involves W and Mo pnictide triple bonds, but several examples of terminal chromium(VI) nitrido complexes have been prepared.[13−15] In contrast, the analogous complexes containing a chromium−phosphorus triple bond have not been reported.

Two trends in the chemistry of group 6 metal Cr, Mo, and W organometallic complexes are relevant here. The number of examples of metal VI complexes increases going down the family column as Mo and W favor higher oxidation states,[16] but the reverse periodic relationship holds with nitrides, phosphides, and arsenides as mentioned above.[1] We have developed a straightforward method to synthesize spectroscopic quantities of simple terminal pnictide complexes through the reaction of laser ablated metal atoms and NF_3 or PF_3. Through insertion and α-F-transfer, this reaction produced all three group 6 N≡MF_3 molecules, P≡MoF_3 and P≡WF_3, but P≡CrF_3 was not formed owing to its higher energy.[17] This reaction was also effective for CHX_3 and CX_4 precursors (X = F, Cl) to form the methylidyne HC≡MX_3 and FC≡MX_3 molecules with metal carbon triple bonds.[18] Here, we employ these methods to the Cr, Mo, and W reactions with AsF_3.

Experimental and Computational Methods

Laser ablated Cr, Mo, and W atoms (Johnson−Matthey) were reacted with AsF_3 (Ozark−Mahoning, vacuum distilled from dry NaF) in excess argon or neon during condensation at 4 K using a closed-cycle refrigerator (Sumitomo Heavy Industries model RDK 205D) as described elsewhere.[19,20] Reagent gas mixtures were typically 0.2 or 1% in neon or argon. After reaction, infrared spectra were recorded at a resolution of 0.5 cm^{-1} using a Nicolet 750 spectrometer with a Hg−Cd−Te B range detector. Samples were later irradiated for 15 min periods by a mercury arc street lamp (175 W) with the globe removed using a combination of optical filters and/or annealed to allow reagent diffusion and further reaction.

Following previous work,[17] complementary density functional theory (DFT) calculations were carried out using the Gaussian 03 package,[21] the B3LYP and BPW91 density functionals,[22] the 6-311+G(3df) basis sets for As and F[23] and the SDD pseudopotential and basis set for the metal atoms[24] in order to provide a consistent set of vibrational frequencies for the reaction products. Geometries were fully relaxed during optimization, and the optimized geometry was confirmed by vibrational analysis. All of the vibrational frequencies were calculated analytically with zero-point energy included for the determination of reaction energies using the B3LYP functional.

More rigorous CASSCF and CASPT2 calculations were performed for the subject molecules.[25,26] The basis set was of VTZP quality with the primitives obtained from the relativistic ANO-RCC basis sets: 6s5p3d1f for As, 5s4p2d1f for P, 4s3p2d1f for F, and 6s5p3d2f1g for Cr, 7s6p4d2f1g for Mo and 9s8p6d4f2g1h for W.[27−29] Scalar relativistic effects are

* Corresponding author. E-mail: lsa@virginia.edu.
[†] University of Virginia.
[‡] University of Lund.

10.1021/jp901308n CCC: $40.75
Published on Web 05/04/2009

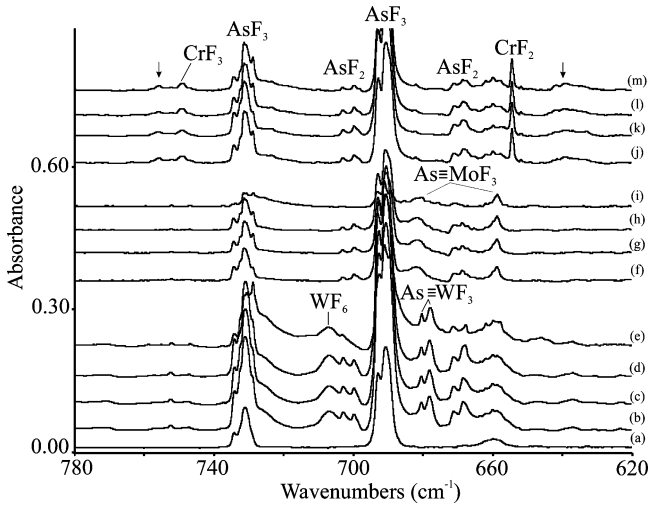

Figure 1. Infrared spectra in the 780 to 620 cm^{-1} region for group 6 metal atom reaction products with AsF_3 in excess argon. (a) Spectrum after deposition of 1% AsF_3 in argon at 5 K for 10 min, (b) spectrum after codeposition of laser-ablated W and AsF_3 at 1% in argon at 5 K for 60 min, (c) spectrum after annealing to 20 K, (d) spectrum after >220 nm irradiation for 20 min, and (e) spectrum after annealing to 35 K. (f−i) Analogous spectra for Mo; (j−m) analogous spectra for Cr.

included in the calculations using the Douglas−Kroll−Hess Hamiltonian as is standard in the MOLCAS software. The active space was chosen to describe the M≡As triple bonds: six active orbitals (three bonding and three antibonding) with six active electrons. All valence electrons, plus the semicore electrons 3s,3p for Cr, 4s, 4p for Mo, 5s, 5p for W, were correlated in the CASPT2 calculations, which used the standard IPEA Hamiltonian and an imaginary shift of 0.1 to remove some weak intruder states. All calculations were performed with the MOLCAS-7 quantum chemistry software.[30] The geometries were optimized at the CASPT2 level and vibrational frequencies were computed using numerical gradients and Hessians. All calculations were performed in C_s symmetry but all molecules converged to C_{3v} symmetry.

Results and Discussion

The reaction products of Cr, Mo, and W atoms with AsF_3 molecules will be characterized by matrix infrared spectra, quantum chemical calculations, and comparison to results from the analogous PF_3 reactions.[17,20] Very strong AsF_3 absorptions were observed at 731 and 691 cm^{-1} in solid argon along with new metal independent bands at 809 and 784 cm^{-1} for AsF_5 and 699.7 and 668.4 cm^{-1} for the AsF_2 free radical.[31,32] We report now new metal dependent product absorptions.

Infrared Spectra. Infrared spectra of the laser-ablated Cr, Mo, and W atom reaction products with AsF_3 in excess argon are compared in Figure 1 and Table 1. Two new absorptions were observed at 755.9 and 639.5 cm^{-1} for chromium. These bands, marked with arrows, increased in concert on near UV irradiation (>320 nm, not shown), but decreased together with higher energy radiation (>220 nm), then increased on final annealing to 30 K. Sharp bands at 654.3 and 749.4 cm^{-1} are due to CrF_2 and CrF_3 based on previous work[32] and their observation as weaker bands in previous PF_3 and stronger bands in analogous NF_3 experiments.[17]

Two new bands were observed for molybdenum, a weak structured band at 682 cm^{-1}, with subpeaks at 685.2, 682.7, 681.7, 680.3, and 678.4 cm^{-1}, and a sharp 658.7 cm^{-1} absorption. These bands are compared with the PF_3 reaction product counterparts in Figure 2. Early annealing and ultraviolet irradiation had little effect on these bands, but they sharpened on final annealing. Any MoF_6 absorption that might be present[17] is covered by the 731 cm^{-1} precursor absorption. Two sharp new bands appeared with tungsten at 680.4 and 678.2 cm^{-1}, which were little effected by annealing or photolysis. A broader band at 707.0 cm^{-1} is assigned to WF_6, based on its observation at 706.7 cm^{-1} in the NF_3 experiments and the high resolution band position of 713.9 cm^{-1} for $^{184}WF_6$.[17,33,34]

Corresponding experiments were also performed in excess neon, and the AsF_2 radical absorptions shifted to 706.0 and 676.0 cm^{-1} just above the argon matrix values. No other products were observed for chromium, and the Mo investigation revealed a broad 690 cm^{-1} and a shoulder 667 cm^{-1} band. The tungsten experiment in neon gave shifted bands at 710.6 (WF_6), 689.7, and 688.2 cm^{-1}.

Calculations. Reactions of AsF_3 with laser-ablated Cr, Mo, and W atoms are expected to proceed through insertion and α-F-transfer following our work with NF_3 and PF_3 in excess argon. DFT calculations were done for the three quintet, triplet, and singlet state steps in reaction 1 for each metal,

$$M + AsF_3 \rightarrow AsF_2{-}MF \rightarrow AsF{=}MF_2 \rightarrow As{\equiv}MF_3 \quad (1)$$

and the energy profile is illustrated in Figure 3. The triplet state arsinidene $AsF{=}CrF_2$ is the lowest energy product for Cr, but the terminal arsenide singlet states are the most stable products for Mo and W. Notice that the tungsten arsenide product is half again more stable than the molybdenum arsenide product.

The terminal arsenides have the C_{3v} symmetry structures shown in Figure 4 using three levels of theory. The hybrid and pure density functionals give almost the same structural parameters; the CASSCF/CASPT2 triple bonds are about 1% longer and the M−F bonds are 1% shorter than the density functional medians.

Calculated frequencies for the As≡MF_3 molecules using three methods are also compared in Table 1. The hybrid density functional frequencies are slightly higher, as expected,[35] than the pure density functional values, and both are lower than the CASSCF/CASPT2 frequencies.

As≡MF_3 Molecules. The major metal dependent products in the Mo and W experiments are identified as terminal metal arsenides from comparison between calculated and observed frequencies as summarized in Table 1. First, our work with NF_3, PF_3, and trihalomethanes[17,18] showed that these reactions proceed through insertion and fluorine transfer steps as outlined in reaction 1 to form the lowest energy As≡MoF_3 and As≡WF_3 molecules, which are exothermic by 102 and 147 kcal/mol for Mo and W, respectively (Figure 3).

It is important to note that the molybdenum natural isotopic profile on the 682 cm^{-1} band (Figure 2) indicates the participation of a single Mo atom in this vibration although the resolution is not as good as with the phosphorus counterpart: the Mo 92−98 separations are the same 4.9 cm^{-1} for these antisymmetric MoF_3 stretching modes.[17] Our B3LYP calculation predicts this isotopic separation as 5.2 cm^{-1}, which is in good agreement, and predicts the separation for the symmetric counterpart as 1.4 cm^{-1}, which is not resolved on the 658.7 cm^{-1} band. The observation of two Mo−F stretching frequencies rules out the higher energy first insertion product $AsF_2{-}MoF$, and the computed Mo−F stretching mode for this first insertion product, 656 cm^{-1}, is lower than our strong 682 cm^{-1} band. The two Mo−F stretching frequencies computed for the second also higher energy $AsF{=}MoF_2$ product at 683 and 649 cm^{-1}

TABLE 1: Observed and Calculated Vibrational Frequencies of the Group 6 As≡MF_3 Molecules in Singlet Ground Electronic States with C_{3v} Structures[a]

Approximate	As≡CrF_3							As≡MoF_3							As≡WF_3						
Description	obs[b]	cal(L)	int	cal(W)	int	cal(C)	int	obs[b]	Cal(L)	int	cal(W)	int	cal(C)	int	obs[b]	cal(L)	int	cal(W)	int	cal(C)	int
M-F, e	n. o.	759	318	750, 744	131, 129	793	456	682	688	290	678	254	698	204	678	673	238	663	210	693	318
M-F, a_1		700	126	678	100	726	167	659	659	117	646	97	681	170	680	670	109	657	90	697	155
M≡As, a_1		468	0	444	0	387	16		428	2	411	2	377	4		389	2	375	2	360	2
F-M-F, e		218	3	210	3	216	31		202	3	197	2	207	11		207	2	203	1	212	6
F-M-F, a_1		206	2	202	0	209	18		186	0	183	30	185	8		185	2	182	2	185	1
As-M-F, e		193	6	186	6	183	10		172	14	171	10	167	12		165	12	166	8	162	10

[a] Frequencies and intensities are in cm^{-1} and km/mol. Frequencies and intensities computed with B3LYP(L), BPW91(W), or CASSCF/CASPT2(C) methods in the harmonic approximation. Symmetry notations are for C_{3v} symmetry. The BPW91 structure for As≡CrF_3 was slightly distorted. [b] Observed in an argon matrix: the instrumental limit is 410 cm^{-1}. Neon matrix counterparts are (Cr) n.o., (Mo) 690, 667 cm^{-1}, and (W) 690, 688 cm^{-1}.

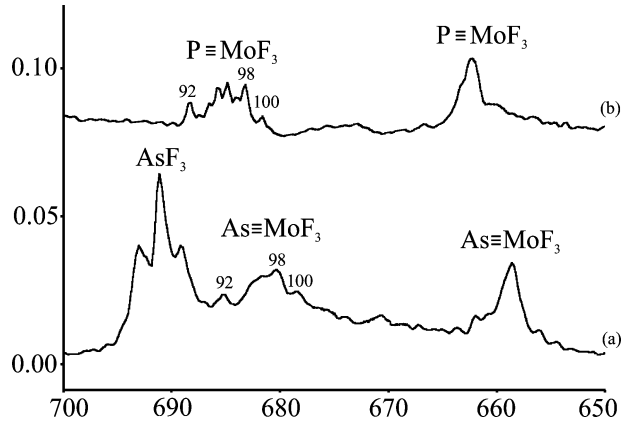

Figure 2. Infrared spectra for natural Mo atom reaction product with PF_3 and AsF_3 in the 690−640 cm^{-1} region using expanded wavenumber scale. (a) Spectrum after codeposition of laser-ablated Mo and AsF_3 at 1% in argon at 4 K for 60 min, > 220 nm irradiation for 20 min, and annealing to 35 K, and (b) spectrum after codeposition of laser-ablated Mo and PF_3 at 0.5% in argon at 4 K for 60 min, > 220 nm irradiation for 20 min, and annealing to 30 K.

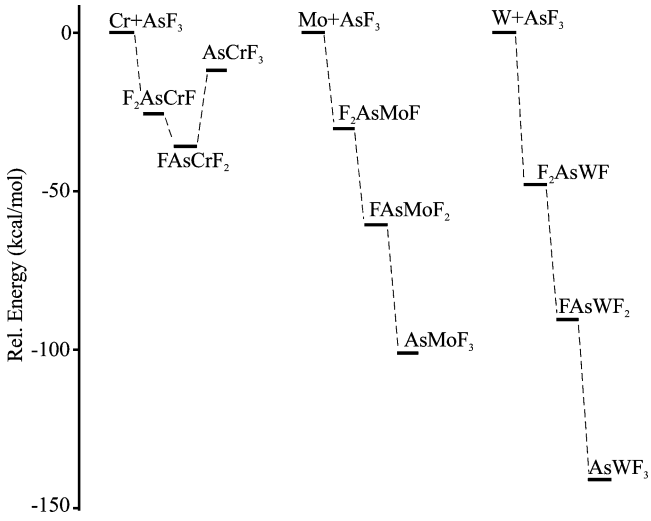

Figure 3. Energy profile of group 6 metal atom and AsF_3 reaction products computed at the B3LYP level of theory relative to the energy of the metal atom and the reagent molecule.

(Table 2) do not correlate with the observed values as well as those for the lowest energy As≡MoF_3 product, as the B3LYP values are usually slightly higher than the observed values. In addition, the As−F stretching mode predicted at 619 cm^{-1} is not observed (region not shown in the figure).

Our calculations using three methods predict the antisymmetric MoF_3 stretching mode higher than the symmetric

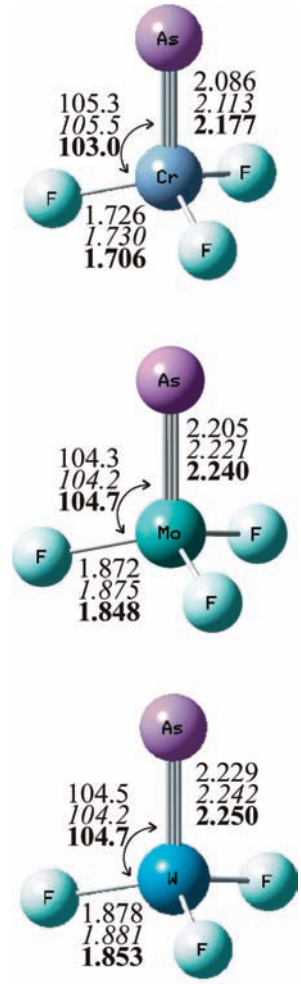

Figure 4. Structures calculated for the group 6 As≡MF_3 molecules in C_{3v} symmetry using B3LYP, *BPW91*, and **CASSCF/CASPT2** methods with parameters given for each method, respectively.

counterpart for As≡MoF_3, as is observed. Furthermore, the frequencies are computed very close to the observed values with B3LYP, namely 6 cm^{-1} higher for the antisymmetric mode and within 1 cm^{-1} for the symmetric mode; the BPW91 values are slightly lower, and the CASPT2 determinations are slightly higher. Since such calculations are not an exact science, the reinforcement of three different methods is reassuring.

The 680.4 and 678.2 cm^{-1} absorptions are assigned to the As≡WF_3 molecule for the following reasons. First, the even higher energy AsF_2−WF and AsF=WF_2 molecules can be ruled out for analogous reasons to those described above. In the case of tungsten, the B3LYP frequencies are slightly lower than the

TABLE 2: Calculated Frequencies of the AsF=MoF_2 and AsF=WF_2 Molecules in the Triplet Ground Electronic States[a]

approximate description	AsF=MoF_2		AsF=WF_2	
	cal(L)	int	cal(L)	int
anti M-F str	683	197	664	158
sym M-F str	650	158	650	64
As−F str	619	121	592	133
As-M str	263	0	281	1
F-M-F bend	146	7	155	4
As−F,M-F def	137	1	147	0
Deformation	120	9	114	4
Deformation	83	7	98	4
Deformation	71	1	59	5

[a] Frequencies and intensities are in cm^{-1} and km/mol. Frequencies and intensities computed with B3LYP(L) method in the harmonic approximation.

observed values, and the computed frequencies for AsF=WF_2 are even lower than those for As≡WF_3 (Tables 1 and 2). Second, the new bands are very near the analogous 683.4 and 680.6 cm^{-1} absorptions for the P≡WF_3 molecule,[17] and third the calculations predict these frequencies with the density functionals slightly lower and the CASPT2 slightly higher. The same relationship was found for N≡WF_3 and P≡WF_3. The CASPT2 method computes the symmetric WF_3 mode 4 cm^{-1} higher with half of the infrared intensity, and the weaker band is observed 2 cm^{-1} higher. Both density functionals predict the intensities correctly but reverse the order of the two modes, which are only 4 cm^{-1} apart. The computed frequencies from these three methods cover the observed bands well enough to sustain our identification of the As≡WF_3 molecule. The observation of WF_6 in these experiments is also supportive of the formation of As≡WF_3. And finally, the neon matrix counterparts about 10 cm^{-1} higher than the argon matrix values are reasonable matrix effects for this molecule[36] and are about the same as that observed for P≡WF_3.

AsF=CrF_2 Molecule. Two bands at 755.9 and 639.7 cm^{-1} in the chromium experiments are reduced on >220 nm irradiation, and they restore on final 30 K annealing. The observation of both CrF_2 and CrF_3 shows that reaction with AsF_3 occurs, but the higher energy As≡CrF_3 molecule is not trapped. Although the 755.9 cm^{-1} band could be due to the strong antisymmetric Cr−F stretching mode for As≡CrF_3, the symmetric mode computed at 700 cm^{-1} (Table 1) was not observed. The stronger band at 755.9 cm^{-1} is not appropriate for the first AsF_2−CrF intermediate, but it correlates well with the calculated value for the strong antisymmetric Cr−F stretching mode of AsF=CrF_2 (Table 3). The weaker symmetric Cr−F mode is masked by CO_2 absorption, and the 639.7 cm^{-1} band fits the computed 642 cm^{-1} value for the As−F stretching mode. Thus, the two new bands in the chromium experiments can be assigned with confidence to the lowest energy arsinidene AsF=CrF_2 product.

TABLE 4: CASPT2 Geometry Parameters for E≡MF_3 Molecules in C_{3v} Symmetry (Bond Distances in Angstroms and Angles in Degrees)[a]

	P≡CrF_3	P≡MoF_3	P≡WF_3	As≡CrF_3	As≡MoF_3	As≡WF_3
R(E≡M)	2.065	2.110	2.131	2.177	2.240	2.250
R(M-F)	1.704	1.851	1.854	1.706	1.848	1.853
<EMF	103.7	103.7	104.6	103.0	103.6	104.4
<FMF	114.5	114.6	113.8	115.0	114.7	114.0
Energy	39	73	103	34	69	67
EBO	2.18	2.67	2.74	1.96	2.60	2.70
X charge	0.25	−0.10	−0.01	0.28	−0.02	0.04
M charge	1.56	1.92	1.80	1.54	1.84	1.75

[a] Computed bond energies (see ref 17 for method of calculation) in kcal/mol and effective bond orders (EBO) for the E≡M bond are also shown together with the Mulliken charges for the E and M atoms.

Structures. The C_{3v} structures computed for terminal arsenide metal trifluoride complexes are illustrated in Figure 4. Structural parameters are given for three theoretical methods, where the CASSCF/CASPT2 (bold type) is expected to be the most accurate. Both density functionals provide structural parameters that are very close to the benchmark CASSCF/CASPT2 values. These parameters are compared in Table 4 along with effective bond orders and Mulliken charges. One might expect the W≡As bond to be longer than the Mo≡As bond, but the difference is only 0.01 to 0.02 Å. The W and Mo ions have similar sizes. This is again illustrated by the M−F bond distances, which differ by only 0.01 Å.

Our calculated parameters can be compared to measurements of such bonds in larger organometallic complexes. Computed values for the present simple complex Mo≡As bond length are comparable to those measured for [(N_3N)Mo≡As], 2.252 Å, and [N(t-Bu)Ar]$_3$Mo≡As, 2.225 Å whereas the 2.290 Å bond length in [(N_3N)W≡As] is slightly longer than our W≡As values (Figure 4).[2,4] A recent density functional theoretical bonding analysis of (MeO)$_3$Mo≡As and (MeO)$_3$W≡As complexes finds 2.224 Å and 2.245 Å bond lengths, which are almost the same, and triple bond σ and π components which are slightly smaller and larger, respectively, than the CASSCF/CASPT2 values reported here for the As≡MoF_3 and As≡WF_3 molecules.[37] Finally, our computed arsenic triple bond lengths for Mo and W are about 2% longer than those taken from tabulated

TABLE 3: Observed and Calculated Frequencies of the AsF_2−CrF and AsF=CrF_2 Molecules in the Quintet and Triplet Ground Electronic States[a]

approximate description	AsF_2−CrF					AsF=CrF_2				
	obs	cal(L)	int	cal(W)	int	obs	cal(L)	int	cal(W)	int
Cr−F str	not obs	689	173	664	151	756	763	204	752	172
As−F, Cr−F str	not obs	647	106	628	90		664	61	661	71
As−F str		633	102	617	87	640	642	141	621	95
Cr−As str		244	3	242	3		254	2	266	2
X−As-F bend		209	1	202	2		156	21	159	14
Deformation		156	16	147	16		137	5	139	2
Deformation		113	2	98	1		119	14	123	10
Deformation		90	3	78	2		96	3	98	3
Deformation		61	9	52i	8		69	27	71	1

[a] Frequencies and intensities are in cm^{-1} and km/mol. Observed in an argon matrix. Frequencies and intensities computed with B3LYP(L) or BPW91(W) methods in the harmonic approximation.

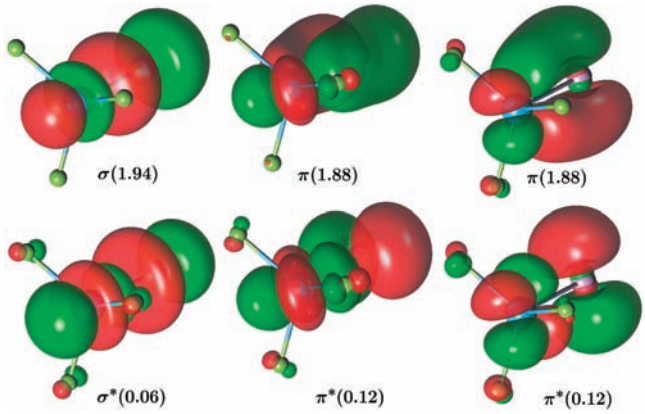

Figure 5. Active bonding and antibonding molecular orbitals for the As≡WF_3 molecule. The contour line used is 0.05 e/au^3. Natural orbital occupation numbers are given below each orbital.

triple bond radii,[38] which is the same relationship found for our computed phosphorus triple bond lengths.[17]

Bonding in Terminal Arsenide and Phosphide Complexes. Rigorous CASSCF/CASPT2 calculations have been employed to analyze the bonding in these simple ternary pnictide complexes. The active molecular orbitals for the As≡MoF_3 and As≡WF_3 molecules are almost identical, and the latter are illustrated in Figure 5. The effective bond order (EBO) is computed as the difference between the total occupation numbers of the bonding and the antibonding orbitals divided by two. The molecular orbital occupations in Figure 5 result in an EBO of 2.70 for As≡WF_3. The corresponding As≡MoF_3 orbital occupancies are σ(1.92), π(1.84), σ^*(0.08), and π^*(0.16), which give an EBO of 2.60, and the computed As≡CrF_3 orbital occupancies are σ(1.80), π(1.58), σ^*(0.19), and π^*(0.42), which give an EBO of 1.96.

The increase in EBO on going down the family group is composed of an increase in the bonding and a decrease in the antibonding orbital occupations, which follows the increase in stability of the highest oxidation state. Natural bond orders are slightly smaller for the arsenide than the phosphide complexes (Table 4) and the more strongly bound nitride complexes described previously.[17] The diffuse 3p orbitals of P do not bind as well with the compact d orbitals of Mo and W, and the more diffuse 4p orbitals of As are even less effective. This is much more pronounced for the hard 3d orbitals of Cr, which do not bind effectively with the larger pnictides. This is shown by lower triple bond dissociation energies (Table 4) and the failure of the reaction to produce the correspondingly higher energy P≡CrF_3 and As≡CrF_3 molecules.

Conclusions

Molybdenum and tungsten atoms react with AsF_3 upon excitation by laser ablation or UV irradiation to form stable trigonal As≡MF_3 terminal arsenides. These molecules are identified by comparison of the closely related infrared spectra of the analogous phosphide species and with frequencies calculated by three theoretical methods. The natural bond orders computed by CASSCF/CASPT2 decrease from 2.67 to 2.60 for P≡MoF_3 to As≡MoF_3 and from 2.74 to 2.70 for P≡WF_3 to As≡WF_3 as the arsenic valence orbitals are less effective than those of phosphorus in bonding to each metal atom, as the larger metal orbital size becomes more compatible with the arsenic valence orbitals, and as the higher oxidation state is more stable.

The chromium reaction gives the lowest energy arsinidene AsF=CrF_2 product instead of the As≡CrF_3 molecule, as the Cr (VI) state is not supported by the softer pnictides.

Acknowledgment. We gratefully acknowledge financial support from NSF Grant CHE 03-52487 and NCSA computing Grant CHE07-0004N to L.A. and from the Swedish Research Council (VR) through the Linnaeus Center of Excellence on Organizing Molecular Matter (OMM) to P.-Å.M. and B.O.R. The AsF_3 sample was kindly provided by G. L. Schrobilgen and M. J. Hughes, and C. C. Cummins sent helpful information.

References and Notes

(1) Balazs, G.; Gregoriades, L. J.; Scheer, M. *Organometallics* **2007**, *26*, 3058, and references therein.
(2) Scheer, M.; Müller, J.; Häser, M. *Angew. Chem., Int. Ed.* **1996**, *35*, 2492.
(3) Mösch-Zanetti, N. C.; Schrock, R. R.; Davis, W. M.; Wanninger, K.; Seidel, S. W.; O'Donoghue, M. B. *J. Am. Chem. Soc.* **1997**, *119*, 11037.
(4) Curley, J. J.; Piro, N. A.; Cummins, C. C., personal communication, 2008.
(5) Gdula, R. L.; Johnson, M. J. A.; Ockwig, N. W. *Inorg. Chem.* **2005**, *44*, 9140.
(6) Gdula, R. L.; Wiedner, E. S.; Johnson, M. J. A. *J. Am. Chem. Soc.* **2006**, *128*, 9614.
(7) Geyer, A. M.; Gdula, R. L.; Wiedner, E. S.; Johnson, M. J. A. *J. Am. Chem. Soc.* **2007**, *129*, 3900.
(8) Laplaza, C. E.; Davis, W. M.; Cummins, C. C. *Angew. Chem., Int. Ed. Engl.* **1995**, *34*, 2042.
(9) Cherry, J. P. F.; Stephens, F. H.; Johnson, M. J. A.; Diaconescu, P. L.; Cummins, C. C. *Inorg. Chem.* **2001**, *40*, 6860.
(10) Stephens, F. H.; Figueroa, J. S.; Diaconescu, P. L.; Cummins, C. C. *J. Am. Chem. Soc.* **2003**, *125*, 9264.
(11) Figueroa, J. S.; Cummins, C. C. *J. Am. Chem. Soc.* **2004**, *126*, 13916.
(12) Fox, A. R.; Clough, C. R.; Piro, N. A.; Cummins, C. C. *Angew. Chem., Int. Ed.* **2007**, *46*, 973.
(13) Odom, A. L.; Cummins, C. C.; Protasiewicz, J. D. *J. Am. Chem. Soc.* **1995**, *117*, 6613.
(14) Odom, A. L.; Cummins, C. C. *Polyhedron* **1998**, *17*, 675.
(15) Odom, A. L.; Cummins, C. C. *Organometallics* **1996**, *15*, 898.
(16) Schrock, R. R. *Chem. Rev.* **2002**, *102*, 145 (review article).
(17) Wang, X.; Andrews, L.; Lindh, R.; Veryazov, V.; Roos, B. O. *J. Phys. Chem. A* **2008**, *112*, 8030.
(18) (a) Lyon, J. T.; Andrews, L. *Organometallics* **2007**, *26*, 2519. (b) Lyon, J. T.; Cho, H.-G.; Andrews, L. *Organometallics* **2007**, *26*, 6373.
(19) (a) Andrews, L.; Citra, A. *Chem. Rev.* **2002**, *102*, 885, and references therein. (b) Andrews, L. *Chem. Soc. Rev.* **2004**, *33*, 123 and references therein.
(20) Andrews, L.; Cho, H.-G. *Organometallics* **2006**, *25*, 4040, and references therein (review article).
(21) Frisch, M. J., et al. *Gaussian 03, Revision D.01*, Gaussian, Inc.: Pittsburgh, PA, 2004.
(22) (a) Becke, A. D. *J. Chem. Phys.* **1993**, *98*, 5648. (b) Lee, C.; Yang, Y.; Parr, R. G. *Phys. Rev. B* **1988**, *37*, 785. (c) Becke, A. D. *Phys. Rev. A* **1988**, *38*, 3098. (d) Perdew, J. P.; Burke, K.; Wang, Y. *Phys. Rev. B* **1996**, *54*, 16533, and references therein. (e) See also Becke, A. D. *J. Chem. Phys.* **1997**, *107*, 8554.
(23) Frisch, M. J.; Pople, J. A.; Binkley, J. S. *J. Chem. Phys.* **1984**, *80*, 3265.
(24) Andrae, D.; Haeussermann, U.; Dolg, M.; Stoll, H.; Preuss, H. *Theor. Chim. Acta* **1990**, *77*, 123.
(25) Roos, B. O. *The Complete Active Space Self-Consistent Field Method and its Applications in Electronic Structure Calculations, Ch. 69*, p 399, in Advances in Chemical Physics; Ab Initio Methods in Quantum Chemistry - II (Ed. Lawley, K. P.), John Wiley & Sons Ltd. (1987).
(26) Andersson, K.; Malmqvist, P.-Å.; Roos, B. O. *J. Chem. Phys.,* **1992**, *96*, 1218.
(27) Roos, B. O.; Lindh, R.; Malmqvist, P.-Å.; Veryazov, V.; Widmark, P.-O. *J. Phys. Chem. A* **2004**, *108*, 2851.
(28) Roos, B. O.; Lindh, R.; Malmqvist, P.-Å.; Veryazov, V.; Widmark, P.-O. *J. Phys. Chem. A* **2005**, *109*, 6575.
(29) Roos, B. O.; Lindh, R.; Malmqvist, P.-Å.; Veryazov, V.; Widmark, P.-O. *Chem. Phys. Lett.* **2005**, *409*, 295.
(30) Karlström, G.; Lindh, R.; Malmqvist, P.-Å.; Roos, B. O.; Ryde, U.; Veryazov, V.; Widmark, P.-O.; Cossi, M.; Schimmelpfennig, B.; Neogrady, P.; Seijo, L. *Comput. Mater. Sci.* **2003**, *28*, 222.
(31) (a) Khider Aljibury, A. J.; Redington, R. L. *J. Chem. Phys.* **1970**, *52*, 453. (b) Brum, J. L.; Hudgens, J. W. *J. Chem. Phys.* **1997**, *106*, 485.
(32) (a) Van Leirsburg, D. A.; DeKock, C. W. *J. Phys. Chem.* **1974**, *78*, 134. (b) Blinova, O. V.; Shklyarik, V. G.; Shcherlie, L. D. *Zh. Fiz. Khim.* **1988**, *62*, 1640 (CrF_2, CrF_3).
(33) Osin, S. B.; Davlyatshin, D. I.; Ogden, J. S. *Zh. Fiz. Khim.* **2001**, *75*, 294.

(34) The strongest IR band for $^{184}WF_6$ is 713.9 cm^{-1} in the gas phase, and the W-182 to W-186 shift or unresolved bandwidth is 1.3 cm^{-1}. Boudon, V.; Rotger, M.; He, Y.; Hollenstein, H.; Quack, M.; Schmitt, U. J. Chem. Phys. 2002, *117*, 3196 (WF_6).

(35) (a) Scott, A. P.; Radom, L. *J. Phys. Chem.* **1996**, *100*, 16502. (b) Andersson, M. P.; Uvdal, P. L. *J. Phys. Chem. A* **2005**, *109*, 2937. (c) von Frantzius, G.; Streubel, R.; Brandhorst, K.; Grunenberg, J. *Organometallics* **2006**, *25*, 118.

(36) Jacox, M. E. *Chem. Phys.* **1994**, *189*, 149.

(37) Pandey, K. K.; Frenking, G. *Eur. J. Inorg. Chem.* **2004**, 4388.

(38) Pyykkö, P.; Riedel, S.; Patzschke, M. *Chem.—Eur. J.* **2005**, *11*, 3511.

JP901308N